ACS APPLIED MATERIALS & INTERFACES

Research Article

www.acsami.org

Surface Modification for Superhydrophilicity and Underwater Superoleophobicity: Applications in Antifog, Underwater Self-Cleaning, and Oil–Water Separation

Kang-Ting Huang,[†,‡] Shiou-Bang Yeh,[†,‡] and Chun-Jen Huang*[,†,§]

[†]Department of Biomedical Sciences and Engineering and [§]Chemical & Materials Engineering Department, National Central University, Jhong-Li, Taoyuan 320, Taiwan

Supporting Information

ABSTRACT: A facile yet effective surface modification strategy for superhydrophilicity and underwater superoleophobicity was developed by silanization of zwitterionic sulfobetaine silane (SBSi) on oxidized surfaces. The coatings exhibit excellent wetting properties, as indicated by static contact angles of <5°, and long-term stability under exposure to heat and UV irradiation. The SBSi-modified surfaces were employed for applications in antifog, self-cleaning, and oil–water separation. The SBSi glasses retained their optical transmittance because of the rapid formation of coalesced water thin films on surfaces in contact with water vapor and moisture. In addition, the underwater–oil contact-angle measurements verified the underwater superoleophobicity of the zwitterionic SBSi coatings. The oil spills on the SBSi coating could be readily removed in contact with water to realize the self-cleaning property. Besides, we modified stainless steel wire meshes with SBSi for oil–water separation. The optimal oil recovery rate for the oil–water mixtures reached >99.5% when using the SBSi-coated meshes with a pore size of 17 μm. More importantly, the water flux with modified meshes achieved 6.5 × 10^7 L/m^2·h·bar, enabling gravity-driven and energy-saving separation. Consequently, we demonstrated the superhydrophilicity and underwater superoleophobicity of SBSi, offering promise in solving technological problems of interfacial fog, oil spills, and oil–water separation and thereby showing great potential in large-scale commercial applications.

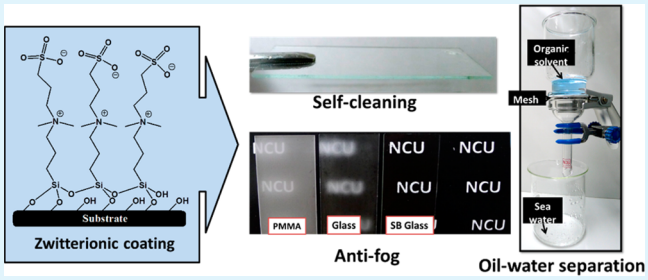

KEYWORDS: *zwitterionic materials, underwater superoleophobicity, silanization, oil–water separation, antifog, self-cleaning*

INTRODUCTION

Alteration of the surface wettability through chemical and/or physical modifications has attracted considerable attention for a wide spectrum of applications. Superhydrophilic and superhydrophobic coatings that present extreme wetting behaviors in particular have been pursued.[1−3] Fundamentally, when a water droplet is brought into contact with a solid surface, interfacial energies balance to a minimum, resulting in a three-phase contact angle (CA), as described by Young's equation.[4] A high energy surface therefore has a lower CA than a low energy surface. Interestingly, the surface coating with either superhydrophilicity or superhydrophobilicity can be applied to the same applications in some cases. Antifog coatings are one such example. Fog forms while a considerable amount of the water droplets are condensed on a transparent substrate, leading to the scattering of visible light. In our daily life, fog appears frequently on eyeglasses, swimming googles, mirrors, optical lens, etc. Surface fog can restrain or weaken the functions of certain instruments, such as IR microscopes, bronchoscopes, and solar cells.[5−7] To remove fog from the surfaces, superhydrophilic coatings were used to allow rapid spreading and coalescence of water droplets to form a pseudofilm. This results in low scattering of incident light and retention of light transmittance.[8−11] Additionally, superhydrophobicity-induced antifog arises from the low adhesion of water droplets on the surfaces, facilitating the repelling of water. The surface therefore stays dry without interference to the light path.[12−14]

The other important application associated with surface wettability is oil–water separation. Oily wastewater produced from industries such as metallurgy, food, and leather has been a major pollutant in the ecological environment. Moreover, because of an increasing number of oil-spill accidents[3] and the wide acceptance of the new mining technique called hydraulic fracking,[2] oil–water separation has become a serious environmental and economic issue. Conventional approaches such as gravity separation, centrifugation, electric field, coagulation, and absorbance have been widely employed in industries for water treatment.[15−17] However, these techniques have low separation efficiency and low cost effectiveness and generate secondary pollutants. Recently, membrane filtration technology has

Received: January 16, 2015
Accepted: September 10, 2015
Published: September 10, 2015

DOI: 10.1021/acsami.5b07362
ACS Appl. Mater. Interfaces 2015, 7, 21021−21029

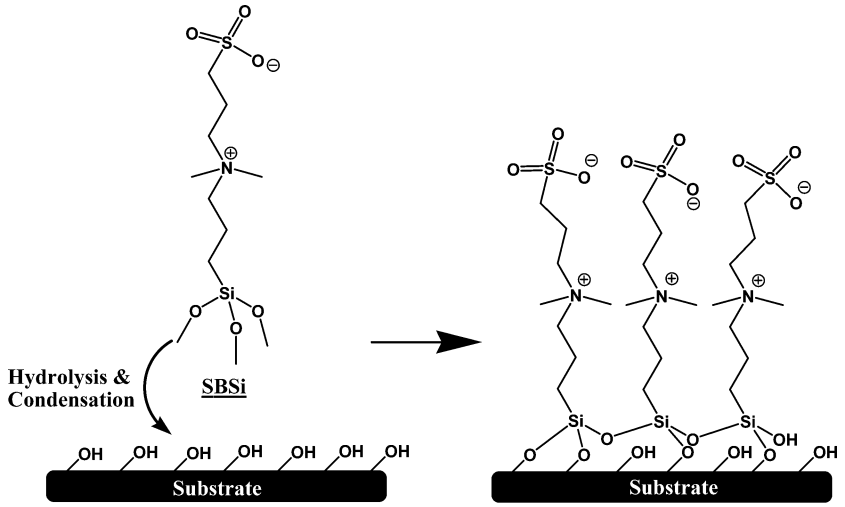

Figure 1. Chemical structure of SBSi and the formation of SBSi coatings on the oxidized substrate.

offered promise in high performance for oil–water separation, in terms of the purification efficiency, selectivity, and mass flux.[18,19] Coatings with superhydrophilicity or superhydrophobicity on the membranes can selectively collect or filter oil from the mixtures. The superhydrophobic membranes permit the oil to go through while water runs off the surface. These filtration devices, however, tend to result in surface contamination with oil, leading to decreases in the separation efficiency and flux.[20] In addition, water generally has higher density than oil, which initially contacts the membranes to form an insulating layer from oil permeation or adsorption. The reverse strategy using superhydrophilic coatings has attracted more attention. Many surface engineering methods have been established, including mineralization with $CaCO_3$,[19] coating with hydrogel,[21] grafting of zwitterionic or ethylene glycol based polymer,[1,4,22] dip-coating with copolymer,[9,23] coating with TiO_2 nanoparticles,[24] and nanowire texturing.[25] These remarkable achievements have been made and successfully met the demanded separation efficiency. However, there is still much potential to be fulfilled for many large-scale industrial applications. The constraining factors in the current approaches include low flow flux, high fabrication cost, low stability, required external energy input (e.g., UV irradiation or pumping), pore plugging by oil droplets, and small-scale production. Moreover, the susceptibility of hydrophilic surfaces to contaminations potentially ruins the oil–water separation properties. Thus, a surface possessing a self-cleaning property is highly desirable for its extended lifetime and applicability.

In this study, we report a facile, low-cost yet robust approach to fabricate superhydrophilic and underwater superoleophobic surfaces on silica glass and stainless steel wire mesh for applications in antifog, self-cleaning, and oil–water separation. The surface coatings were readily prepared by silanization with zwitterionic sulfobetaine silane (SBSi; Figure 1). The CA measurements on SBSi-modified surfaces by water in air and organic fluids in water were carried out to demonstrate the surface wettability. The stability of SBSi coatings was confirmed by long-term exposure to heat and UV light. The influence of the surface wettability and fog formation on the optical transparence of substrates was investigated. Moreover, the self-cleaning property of the SBSi-modified substrates was demonstrated by the removal of adsorbed soybean oil in contact with water. For the separation of oil–water emulsions, the flow flux and recovery rate of the SBSi-modified stainless steel wire meshes were evaluated. In addition to the proof-of-concept, it is imperative to develop a suitable and cost-effective surface engineering method for industrial applications. Thus, we believe that the SBSi coating holds great potential for the various needs associated with superhydrophilicity and underwater superoleophobicity.

MATERIALS AND METHODS

Materials. Standard glass microscope slides (Green cross mesical), hexane (Burdick & Jackson), ethyl ether (ECHO Chemical), toluene (Fisher Scientific), synthetic sea salt (Eco-marine, Taiwan), sodium dodecyl sulfate (SDS; Sigma-Aldrich), and Tween 80 (Sigma-Aldrich) were used as received. Ethanol (anhydrous, ECHO Chemical) was used in the surface modification process. Deionized (DI) water and acetone (99.5% anhydrous, ECHO Chemical) were used as a washing solution during the procedures. Gasoline (RON 95) and diesel were purchased from CPC Corp., Taiwan. Soybean oil was purchased from Taiwan Sugar Corp. [(*N*,*N*-Dimethylamino)propyl]trimethoxysilane (DMASi) was purchased from Gelest Inc. 1,3-Propane sultone was purchased from Alfa Aesar.

Synthesis of SBSi. SBSi was synthesized as described in the previous report.[26,27] Briefly, 5 g of DMASi (24 mmol) and 3 g of 1,3-propane sultone (25 mmol) were dissolved in 25 mL of anhydrous acetone and reacted for 6 h under nitrogen protection at room temperature. The mixture was filtered with a G4 glass Gooch filter. The white product on the filter was washed with anhydrous acetone, followed by drying under reduced pressure and collection. The white powder compound (5.1 g) was obtained with a yield of 64.2%.

Surface Modification with SBSi. The standard glass microscope slides and cut 304 stainless steel mesh were first washed with solutions in a sequence of 10% SDS solution, DI water, and acetone. A 10 min sonication was performed for each step. The samples were then treated with oxygen plasma (Harrick air-plasma cleaner, PDC-32G) at a power of 18 W and a vacuum level of 0.3 Torr for 5 min. The oxidized samples were immediately dipped in a solution containing 5 mM SBSi in ethanol with 0.2% (v/v) DI water to accelerate hydrolysis of methylsilane. After 12 h of incubation at room temperature, the samples were washed by a 10 min sonication in ethanol to remove the unreacted SBSi. Finally, the samples were cured at 80 °C for 1 h for condensation of the silane group on the substrate surface (Figure 1).

X-ray Photoelectron Spectroscopy (XPS) Characterization. The chemical composition of the glass surfaces and 304 stainless steel modified with SBSi was determined by XPS (VG Sigma Probe, Thermo VG-Scientific). The measurements were performed with a spectrometer equipped with an Al Kα excitation source (25 W, 15 μm) in a vacuum of 2×10^{-8} Pa. The XPS spectra were acquired with a

DOI: 10.1021/acsami.5b07362
ACS Appl. Mater. Interfaces 2015, 7, 21021–21029

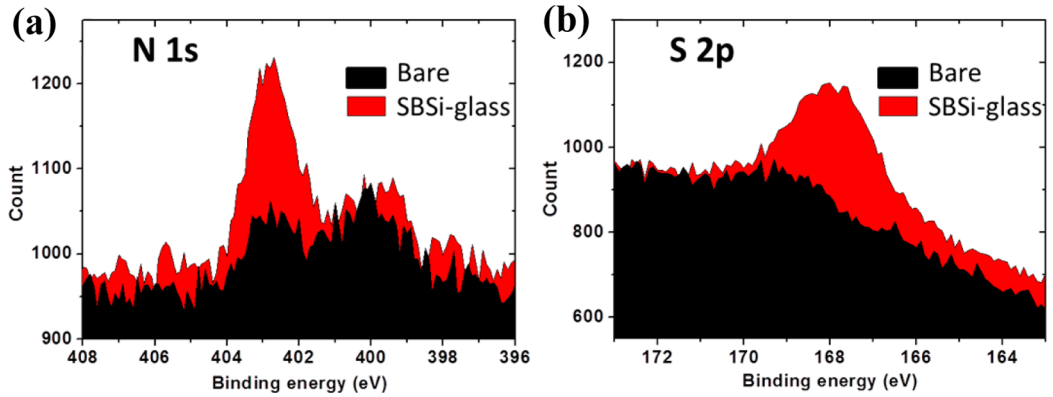

Figure 2. XPS spectra of N 1s (a) and S 2p (b) for the bare glass and SBSi-glass.

pass energy of 58.8 eV. The binding energy (BE) was estimated to be accurate within 0.2 eV.

CA Measurements. In-air water and underwater−oil CAs were measured via the sessile-drop method using an optical CA goniometry (Phoenix mini, Surface Electro Optics). A cell containing a prism stand was used for the underwater measurements. The droplets used were 5 μL from a microsyringe, and the measurements were performed at least three times at random positions on a sample.

Antifogging and Self-Cleaning Tests. Poly(methyl methacrylate) (PMMA), quartz glass, and SBSi-modified quartz glass were used in the experiments. The levels of fogging on the samples were quantified with a UV−vis spectrophotometer (V-630, Jasco) at 480 nm after pretreatment with 100% relative humidity above boiling water for 30 s or −20 °C in a refrigerator for 5 min. It took approximately 5 s to transfer the samples into the spectrophotometer and begin the measurements.

Scanning Electron Microscopy (SEM) Imaging. SEM images were taken on a low-vacuum scanning electron microscope (S-3500N, Hitachi) to observe the morphologies of the stainless steel meshes.

Water-Flux Measurement. Freshly prepared synthetic seawater was prepared for the water-flux measurements with the meshes. The flux (f) was determined using the following equation:

$$f = V/atp \quad (1)$$

where V is the volume of the permeate (L), a is the valid area of the membrane (m^2), t is the testing time (h), and p is the pressure drop (bar). The testing pressure drops for the oil−water separations are listed in Table S1. Gravity was the only driving force during filtration.

Oil−Water Separation. Organic fluids of ether, toluene, hexane, gasoline, diesel, and soybean oil were used for oil−water separation to determine the recovery rates. The contents of the synthetic seawater are shown in Table S2. The samples for oil−water separation were prepared in two ways: directly mixing organic fluids and seawater by shaking the solutions at 250 rpm for 10 min and emulsifying oil−water samples by adding the surfactant Tween 80 at a concentration of 0.5 ppm. The samples were defined according to their preparation methods. A total of 10 mL of synthetic seawater was first poured into the filtration apparatus to hydrate the stainless steel mesh. For each test, a 60 mL sample [1:1 (v/v) oil/seawater] was poured into the filter to be separated. The separation results were recorded with a digital camera (LX5, Lumix, Panasonic). The recovery rates of the organic fluids were quantitatively determined as the ratio of the residue oil volume to the initial oil volume in the mixtures or emulsions. The residue volume was estimated when no dripping was found from the filter.

Aging Test under Exposure to Heat and UV. The stability of SBSi coatings on the glass substrates was carried out by continuous exposure to heat and UV for 144 h. The heat treatment was set at 60 °C in an oven. The UV source (3UV-36uvLamp, 6 W) was set at a wavelength of 365 nm, and the distance between the UV source and samples was kept at 0.8 cm. The stability results were tested by measuring their static in-air water CAs and the recovery rates for oil−water separation.

RESULTS AND DISCUSSION

Surface Modification and Characterization. The glass substrates were silanized with SBSi in an ethanol solution after O_2 plasma treatment. The stable oxane bonds between the silane and substrate formed after baking (Figure 1). The surface chemical composition of the SBSi-modified glass substrate (denoted as SBSi-glass) was confirmed using XPS. XPS spectra for the N and S atoms in the samples were observed (Figure 2). The N peak components with a BE of 402.5 eV appeared in the XPS N 1s core-level spectra, which is associated with quaternary ammonium [$-\underline{N}(CH_3)_3^+$].[27−29] Moreover, spin−orbit split doublets at BEs of 167.0 and 168.2 eV were observed in the S 2p core-level spectra, which are attributed to the sulfonate $C\underline{S}O_3^-$ species (Figure 2b), indicating the presence of SB zwitterions on the glass substrate.[27−29]

The wettability of the SBSi-glass was characterized by the in-air water CA measurement, as shown in Figure 3. The CA of the bare glass was 33°, while the wettability of the SBSi-glass was indicated by a very low CA (CA < 5°), as shown in the CA images (Figure 3a). The presence of the highly polar SB moieties is attributable to the strong interaction with water through ionic solvation, in agreement with other works with zwitterionic materials.[4,22,30−32] Besides, we tested the stability of the SBSi films by scratching the SBSi-glass by an 2H pencil and aging the substrates in long-term storage at room temperature, under exposure to high temperature or UV irradiation. The results indicated that the hydrophilicity of SBSi coatings was substantially maintained after abrasion by the 2H pencil, and the slight increase in the CA can be attributed to contamination of the carbon crumbs, indicating good mechanical stability of the SBSi coatings on glass (Figure S1). In addition, the wettability of SBSi coatings was not affected by the adverse conditions of long-term storage, high temperature, and UV irradiation, as shown by the ultralow CAs in Figure 3a. Therefore, the robust stability of the SBSi coatings allows their applicability under aggressive conditions for a long period of time.

The underwater oleophobicity of SBSi-glasses are revealed by oil contact angles (OCAs) in Figure 3b,c. The substrates were placed in water, and droplets, including air bubbles, ether, toluene, hexane, gasoline, diesel and soybean oil, were introduced to contact with substrates, as shown in Figure 3b. The quantitative estimation of OCAs for bare glass and SBSi-glass is presented in Figure 3c. The OCAs with air bubbles,

DOI: 10.1021/acsami.5b07362
ACS Appl. Mater. Interfaces 2015, 7, 21021−21029

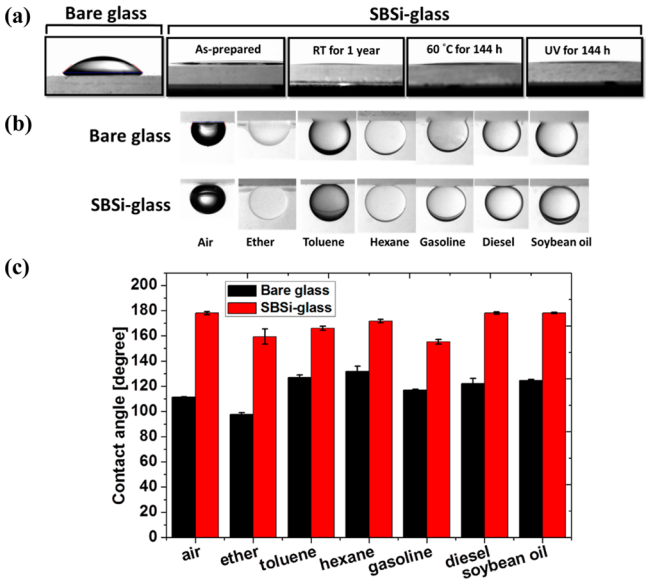

Figure 3. CA measurements for bare and SBSi-glass substrates: (a) in-air water CAs measured for the bare glass and SBSi-glass before and after aging treatments; (b) optical images of the underwater−oil CA measurements for SBSi-glass performed with air bubbles, ether, toluene, hexane, gasoline, diesel, and soybean oil; (c) quantitative results of OCAs for bare and SBSi-glass samples.

diesel, and soybean oil on SBSi-glass are nearly 180°. The OCAs of the organic fluids follow the order of ether < toluene < hexane, which is reversely in accordance with their polarities (the dielectric constants of ether, toluene, and hexane are 4.34, 2.38, and 1.88, respectively). The OCAs of gasoline, diesel, and soybean oil are well correlated with their contents of long carbon chains. In addition, the underwater−oil rolling angles on SBSi-glass were estimated with ether, toluene, hexane, gasoline, and diesel, and the order of the angles obeyed their polarities, as found in the OCA measurements (Figure S2). The low rolling angles (<2.5°) for all organic droplets also indicated their low adhesion to SBSi coatings in water.

The wetting characteristic of the zwitterionic materials strongly relies on the strong interaction between materials and water molecules, resulting in a tightly bound water layer at the interface. This water layer serves as a barrier to adsorption of approaching objectives. Increasing attention is being paid to the application of zwitterionic materials in antibiofouling, which is particularly useful under complex conditions, such as serum and plasma.[32−36] SBSi has been applied to silica, metallic oxide, or silicone to effectively prevent nonspecific adsorption of proteins, bacteria, and lipids.[26,27,37,38] The works demonstrated unique hydration of zwitterionic materials for practical utilization. Herein, detailed studies on the wettability and aging tests for SBSi coatings were carried out. The results show greatly improved interfacial hydrophilicity and underwater oleophobicity by simple and stable silanization. The strong water−substrate interaction through SBSi modification is comparable with that prepared by depositing TiO_2 under UV-light illumination,[25,39] grafting with zwitterionic polymers[4,22] and hydrophilic polymers,[12] and nanotexturing.[25] Moreover, the effect of the roughness change after SBSi modification on the surface wetting can be neglected because the hysteresis in the CA measurements was insignificant (Figure S3).

Antifogging Property. In Figure 4a, water was sprayed on substrates of PMMA (CA = 78°), bare glass, and SBSi-glass,

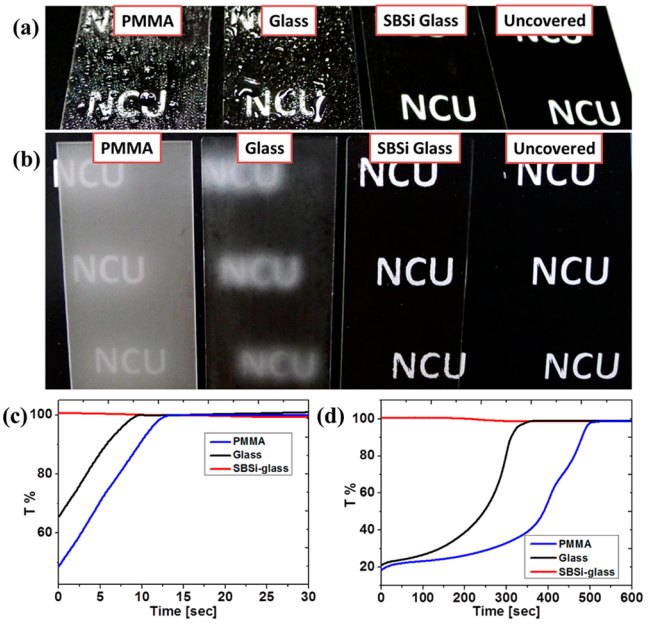

Figure 4. (a) Water spray on samples of PMMA, bare glass, and SBSi-glass. (b) Antifogging test by treating the water steam to samples of PMMA, bare glass, and SBSi-glass. The samples were placed on a paper with letters of "NCU". Light transmission through the samples of PMMA, bare glass, and SBSi-glass after the treatments of hot steam (c) or freezing at −20 °C (d).

which were placed on a paper with letters of "NCU". The images of wetted substrates were recorded with a digital camera. Evidently, the transparency of the SBSi-glass was retained, as indicated by clear letters underneath. On the contrary, a large number of water droplets accumulated on the other substrates to interfere with the light path, leading to visually distorted letters. Moreover, to test the antifogging property of the SBSi-glass, we left the samples in a refrigerator or above boiling water and then moved them to an ambient environment, analogous to the fog-forming conditions. As shown in Figure 4b, after exposure to steam, the water vapor condensed on the SBSi-glass and again formed a pseudofilm without light scattering occurring. However, on the hydrophobic surfaces of PMMA and bare glass, small water droplets influenced the transparency, leading to smearing of the letters beneath.

The UV−vis spectrometer was used to examine the recovery of the substrate transparency in the ambient environment following the freezing or steam treatment. The transmittance to light with a wavelength of 480 nm was monitored as a function of time (Figure 4c,d). Note that the duration of transferring the samples to the UV−vis spectrometer from the treatments was approximately 5 s. We observed that the fog on the SBSi-glass disappeared during transference, which is speculated to provide sufficient time for the spreading and coalescence of water droplets to form a pseudofilm. The relative transmittance of samples was normalized and averaged to that without any treatment. It is remarkable that, after the measurements were started, the transparency of the SBSi-glass was not affected by the freezing and steam treatments. Contrarily, the recovery times for PMMA were 520 and 12.5 s after freezing and steam

DOI: 10.1021/acsami.5b07362
ACS Appl. Mater. Interfaces 2015, 7, 21021−21029

treatments, respectively, and for bare glass, they were 350 and 9 s. Thus, the recovery times were strongly associated with the size of the adsorbed water droplets and the interfacial wettability of the substrates. Because of the superhydrophilicity of the SBSi coatings, the water droplets can quickly coalesce to become a pseudofilm to avoid the scattering of light.

Self-Cleaning Property. To verify the underwater self-cleaning property, we stained bare glass and SBSi-glass with soybean oil and then dipped them into water. The two series of time-sequenced optical images are given in Figure 5a. Although being partly removed, some oil still remained on the bare glass after 3 s of immersion. On the contrary, oil can be thoroughly detached from the SBSi coating in 1.5 s. The substrates were removed from the water, and the images showed no oil stain on the SBSi-glass (Figure 5b). Thus, the SBSi coating presents a superior repellence to oil underwater because of its low adhesion to organic fluids, in accordance with the measurements of underwater OCAs (Figure 3b,c) and rolling water angles (Figure S2).

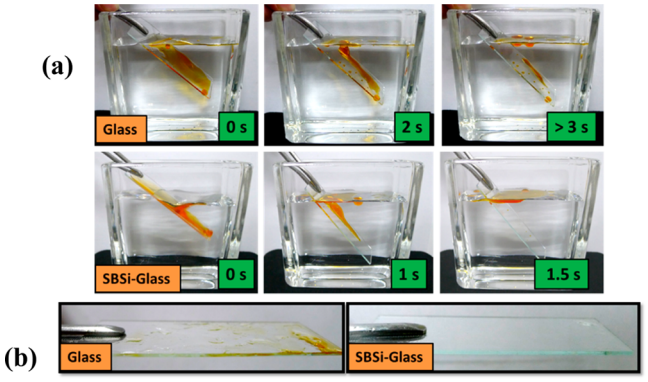

Figure 5. (a) Time-sequenced optical images for detachment of soybean oil from bare glass and SBSi-glass. (b) Images of spilled bare glass and SBSi-glass after water rinsing.

Surface Modification for Stainless Steel Wire Mesh. The stainless steel wire mesh was modified with SBSi following the O_2 plasma treatment to generate hydroxyl groups for the efficient bonding of silane onto the surface.[40] XPS was used to prove the SBSi modification. Parts a and b of Figure 6 show the XPS spectra before and after modification. As with the previous finding with glass modification, the N and S peaks indicate the presence of quaternary ammonium $[-\underline{N}(CH_3)_3^+]$ and sulfonate $(C\underline{S}O_3^-)$ species. The SEM images of bare and SBSi-modified meshes at low and high magnifications in Figure 6c display similar surface topographies. Three meshes with different pore sizes were used for SBSi modification to conduct oil−water separation. The average pore diameters for 300, 500, and 1000 meshes are 55, 33, and 17 μm, respectively. It is apparent that the meshes were homogeneously covered with SBSi, as indicated by the microscopically featureless coatings, and their pore sizes were not affected by modification. Moreover, to confirm the surface wetting property of the meshes after SBSi modification, the underwater OCAs were performed with

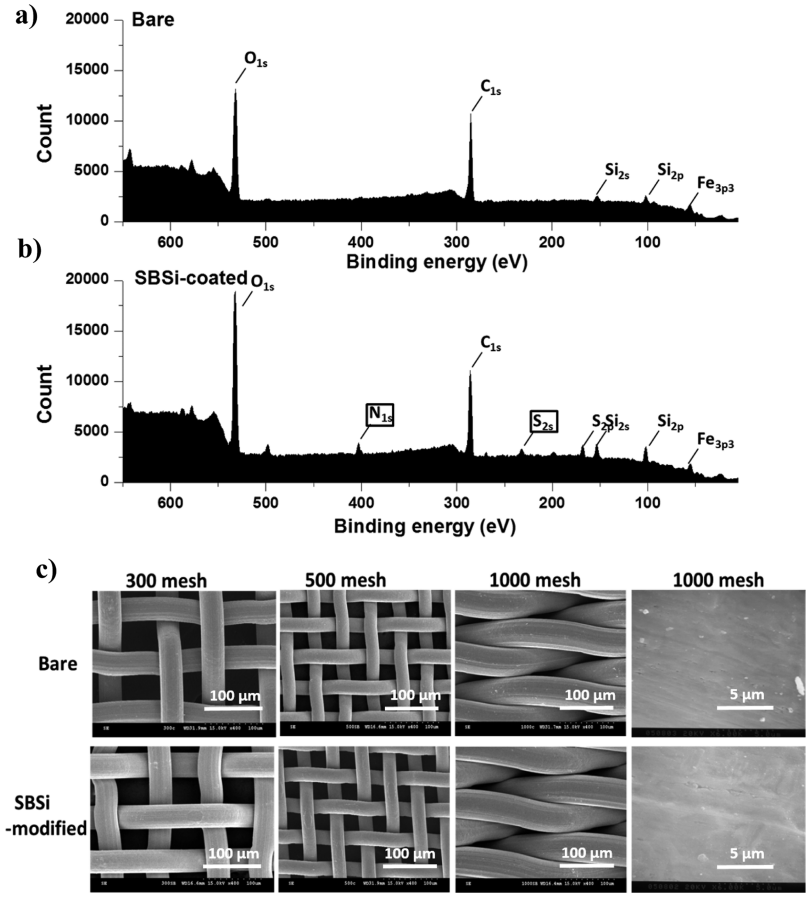

Figure 6. XPS wide-scan spectra for stainless steel wire meshes before (a) and after (b) SBSi modification. (c) SEM images of meshes with different pore sizes of 300, 500, and 1000 mesh. The images show the meshes without (upper row) and with (lower row) SBSi modification.

DOI: 10.1021/acsami.5b07362
ACS Appl. Mater. Interfaces 2015, 7, 21021−21029

ether, toluene, and hexane in comparison with bare and O_2-plasma-treated meshes. In Figure 7, the OCAs of SBSi-coated

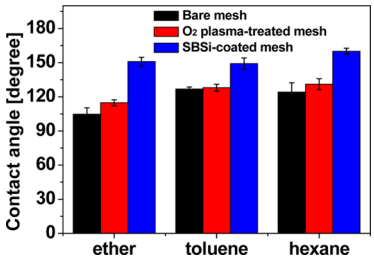

Figure 7. Underwater OCAs of bare, O_2-plasma-treated, and SBSi-coated meshes. The measurements were carried out with ether, toluene, and hexane. The quantitative results of OCAs were obtained from at least three measurements at random mesh positions.

meshes were all above 150°, which were higher than those from bare and O_2-plasma-treated meshes. The results indicate that the success of SBSi modification onto the stainless steel meshes is in agreement with the previous work.[41] Nevertheless, because of the texture of the mesh, the OCAs were not comparable with those of the planar glass surfaces in Figure 3c. Moreover, the aging tests were applied to modified meshes, and the stability of the SBSi coatings on the meshes was evaluated by determining the performance of oil−water separation for mixtures of ether, toluene, and hexane in water. The aging procedures were the same as those for the glasses in Figure 3a, in which the SBSi-coated meshes were exposed to 60 °C and UV irradiation for 144 h. The effectiveness of the aged SBSi-coated meshes for oil−water separation was examined by monitoring the oil recovery rates. As shown in Figure S4, the oil recovery rates did not obviously change after the aging tests, which can demonstrate the good stability of the SBSi coatings on meshes to allow good performance in oil−water separation.

Oil−Water Separation. The permeation fluxes of bare and SBSi-modified meshes for DI water and seawater were experimentally evaluated according to eq 1 (Figure 8). The flow was only driven by the gravity of the fluids. Meshes of different pore sizes were used for testing. In general, the fluxes decreased with increasing pore sizes, in accordance with classical fluid dynamic theory. The Hagen−Poiseuille equation was described as

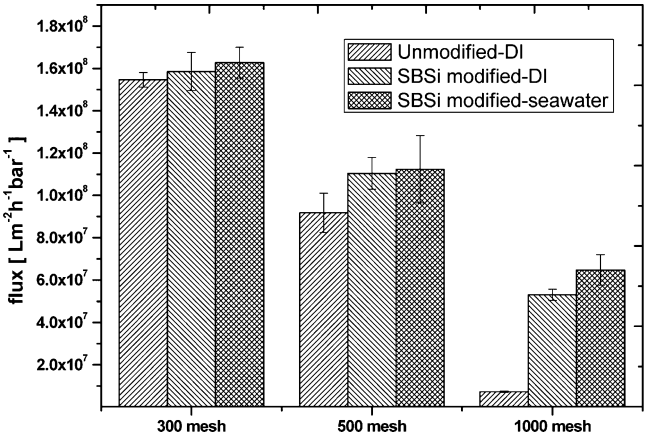

Figure 8. Fluxes of DI water and seawater with 300, 500, and 1000 meshes with and without SBSi modification.

$$J = \varepsilon \pi r_p^2 \Delta p / 8 \mu L \quad (2)$$

where the flux J is interpreted as a function of the surface porosity ε, the membrane pore radius r_p, the pressure drop Δp, the viscosity of the liquid μ, and the total distance L of the liquid running through the membrane. This equation predicts that the filtration flux is directly proportional to the square of the pore size.[42] Besides, it seems tha the flux of the SBSi-modified mesh was higher than that of the bare mesh, especially for the 1000 mesh. This can be ascribed to the high surface wettability of the SBSi coatings, enabling reduction of the shear stress applied to the surfaces and also elevation of the capillary effect on the flow rate. Moreover, the effect of the ionic strength on the permeation flux was marginal, although hydration of the zwitterionic materials was induced by ions in the solution.[43,44] As a result, in this filtration system, the flux is namely governed by the pore size and surface chemistry of the meshes. Note that the flux of the 1000 mesh with SBSi modification was 5.3×10^7 L/m^2·h·bar for DI water, which is more than 3 orders of magnitude higher than that published in previous works.[4,25] Accordingly, a gravity-driven and energy-saving separation process for oil−water mixtures can be realized by using SBSi coatings, and it is in accordance with today's industrial practices.

The 1000 mesh was chosen for oil−water separation to effectively stop the permeation of oil droplets with its small mesh pores. Because of the frequent occurrence of oil spills in marine areas, a filter to rapidly collect a large amount of dispersed oil from the sea surface is highly desirable. In this work, we prepared spilled seawater to verify the performance of SBSi-coated meshes in oil−water separation. The separation apparatus is shown in Figure 9a. The mesh with SBSi

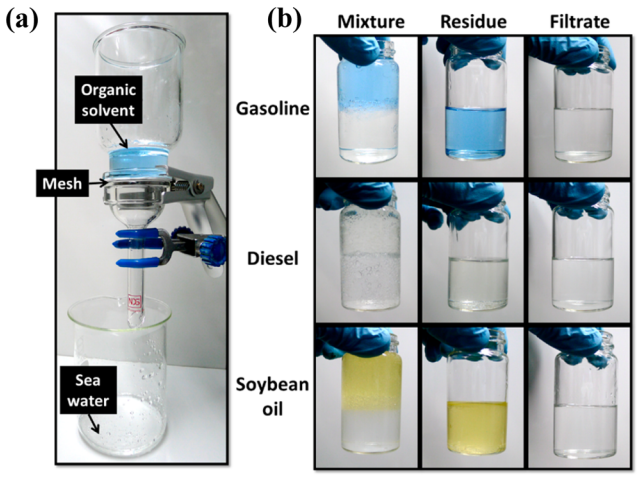

Figure 9. (a) Oil−water separation apparatus. (b) Images of oil−water mixtures, residues, and filtrates in vials before and after separation. The colors of organic fluids are original, without pigment added.

modification was fixed between the top beaker and the bottom funnel. The 30 mL organic fluids of gasoline, diesel, and soybean oil were directly mixed with 30 mL of seawater. The mixtures were separately poured into the beaker for separation. Because of the underwater superoleophobicity of SBSi coatings, the water in the mixtures immediately flowed through the meshes, while the oil stayed above the meshes. The residue and filtrate were individually collected in vials. As shown in the

DOI: 10.1021/acsami.5b07362
ACS Appl. Mater. Interfaces 2015, 7, 21021−21029

photograph (Figure 9b), no visible water and oil were observed in the collected oil and seawater, respectively.

The bare and SBSi-modified 1000 meshes were used for oil−water separation for organic fluids, including ether, toluene, hexane, gasoline, diesel, and soybean oil, from seawater. Two types of samples were prepared: one was oil−water mixtures, and the other was oil−water emulsions, containing a Tween 80 surfactant to stabilize the oil droplets in seawater. In Figure 10a,

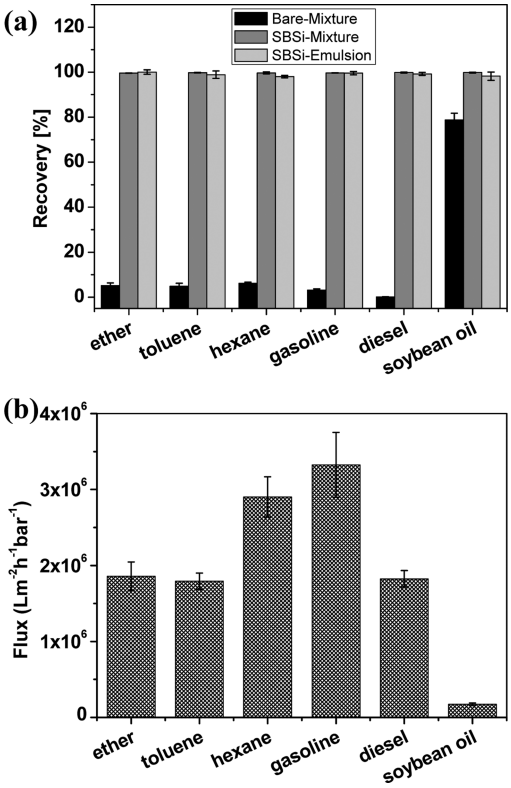

Figure 10. (a) Recovery rates of ether, toluene, hexane, gasoline, diesel, and soybean oil from oil−water mixtures and emulsions using bare and SBSi-modified meshes. (b) Fluxes of water from the oil−water-emulsified solutions, prepared from ether, toluene, hexane, gasoline, diesel, and soybean oil, with SBSi-modified 1000 meshes.

the recovery rates of the organic fluids were quantitatively determined as the ratio of the residue oil volume to the initial oil volume. It is evident that the recovery rates of SBSi-modified meshes (>99.5% for the mixtures and >98.2% for emulsions) were higher than those with bare meshes. This shows that the bare mesh is unable to stop oil from passing through, leading to the low oil recovery rate. The high recovery rate with the bare mesh for soybean oil should be attributed to the high viscosity and the high oil−water interfacial tension, leading to the high oil breakthrough pressure.[19] The fluxes of the SBSi-modified 1000 meshes for the oil−water emulsified solutions varied from 3.3×10^6 to 1.7×10^5 L/m^2·h·bar (Figure 10b), which is lower than that for DI water and seawater (Figure 8). The low fluxes were very likely due to clogging of the mesh pores by oil droplets, in particular for the soybean oil emulsion. In addition, the measurements of the total organic contents (TOCs) for the filtrates reveal high TOC values for ether (TOC = 73 mg/L) and diesel (TOC = 41 mg/L) (Figure S5). Future improvement for better oil cleanliness is to use SBSi-coated meshes with smaller pore sizes to block small oil droplets from passing through. Nevertheless, the mesh still provides a quick separation method for complex emulsion and practical applications in crude filtration. As a result, SBSi-modified mesh holds great promise in oil−water separation and recovery for rapid and efficient oil-spill cleanup in marine environments.

CONCLUSIONS

We proposed a facile and effective coating strategy using zwitterionic SBSi for superhydrophilicity and underwater superoleophobicity for antifog, self-cleaning, and oil−water separation applications. The SBSi coatings allow rapid coalescence of water droplets to form pseudofilms, avoiding the interference of light transmittance and fog formation. Because of the strong water−substrate interaction, the organic fluids spilled on the SBSi-modified substrates could be removed immediately when the substrates are dipped into water. Further, the SBSi-coated stainless steel meshes realized excellent gravity-driven separation processes for oil−water mixtures and emulsions with high flux and oil recovery efficiency. Besides, the stability of the SBSi coatings was confirmed by CA measurements after the aging tests by exposure to heat and UV irradiation, allowing long-term use. Consequently, the modification technology with SBSi has a wide range of applications and holds great potential in industrial practice.

ASSOCIATED CONTENT

Supporting Information

The Supporting Information is available free of charge on the ACS Publications website at DOI: 10.1021/acsami.5b07362.

Pressure drop (Δp) for the flux estimation of the oil-in-water mixtures (Table S1), contents of the synthetic seawater (Table S2), in-air water CAs for samples with 2H pencil scratch treatments (Figure S1), underwater−oil rolling-angle measurements (Figure S2), atomic force microscopy (AFM) image of the unmodified glass and the advancing/receding CA measurement (Figure S3), effectiveness of the oil−water separation of the mixtures on aging meshes (Figure S4), and total organic carbon measurements (Figure S5) (PDF)

AUTHOR INFORMATION

Corresponding Author

*E-mail: cjhuang@ncu.edu.tw (C.-J.H.).

Author Contributions

‡K.-T.H. and S.-B.Y. contributed equally to the work.

Notes

The authors declare no competing financial interest.

ACKNOWLEDGMENTS

The authors acknowledge the Ministry of Science and Technology (MOST 103-2221-E-008-032) and the Center for Dynamical Biomarkers and Translational Medicine, National Central University (NSC 101-2911-1-008-001) for financial support of this project. Profs. Shueh-Lin Yau and Heng-Kwong Tsao from National Central University were acknowledged for the AFM and rolling-angle measurements. We thank Chen Liu from the Taiyuan University of Technology for experimental assistance.

DOI: 10.1021/acsami.5b07362
ACS Appl. Mater. Interfaces 2015, 7, 21021−21029

REFERENCES

(1) Miller, D. J.; Kasemset, S.; Wang, L.; Paul, D. R.; Freeman, B. D. Constant Flux Crossflow Filtration Evaluation of Surface-Modified Fouling-Resistant Membranes. *J. Membr. Sci.* **2014**, *452*, 171−183.

(2) Nicot, J. P.; Duncan, I. J. Common Attributes of Hydraulically Fractured Oil and Gas Production and CO2 Geological Sequestration. *Greenhouse Gases: Sci. Technol.* **2012**, *2* (5), 352−368.

(3) Ketkar, K. W.; Babu, A. J. G. An Analysis of Oil Spills from Vessel Traffic Accidents. *Transport. Res. Part D-Transport. Environ.* **1997**, *2* (1), 35−41.

(4) Zhu, Y. Z.; Zhang, F.; Wang, D.; Pei, X. F.; Zhang, W. B.; Jin, J. A Novel Zwitterionic Polyelectrolyte Grafted PVDF Membrane for Thoroughly Separating Oil from Water with Ultrahigh Efficiency. *J. Mater. Chem. A* **2013**, *1* (18), 5758−5765.

(5) Gao, X. F.; Yan, X.; Yao, X.; Xu, L.; Zhang, K.; Zhang, J. H.; Yang, B.; Jiang, L. The Dry-Style Antifogging Properties of Mosquito Compound Eyes and Artificial Analogues Prepared by Soft Lithography. *Adv. Mater.* **2007**, *19* (17), 2213−2217.

(6) Chen, Y.; Zhang, Y. B.; Shi, L.; Li, J.; Xin, Y.; Yang, T. T.; Guo, Z. G. Transparent Superhydrophobic/Superhydrophilic Coatings for Self-Cleaning and Anti-Fogging. *Appl. Phys. Lett.* **2012**, *101* (3), 033701−033704.

(7) Kim, J. G.; Choi, H. J.; Park, K. C.; Cohen, R. E.; McKinley, G. H.; Barbastathis, G. Multifunctional Inverted Nanocone Arrays for Non-Wetting, Self-Cleaning Transparent Surface with High Mechanical Robustness. *Small* **2014**, *10* (12), 2487−2494.

(8) Oguri, K.; Iwataka, N.; Tonegawa, A.; Hirose, Y.; Takayama, K.; Nishi, Y. Misting-Free Diamond Surface Created by Sheet Electron Beam Irradiation. *J. Mater. Res.* **2001**, *16* (2), 553−557.

(9) Leonard, R. L.; Terekhov, A. Y.; Thompson, C.; Erck, R. A.; Johnson, J. A. Antifog Coating for Bronchoscope Lens. *Surf. Eng.* **2012**, *28* (6), 468−472.

(10) Briscoe, B. J.; Galvin, K. P. The Effect of Surface Fog on the Transmittance of Light. *Sol. Energy* **1991**, *46* (4), 191−197.

(11) Lee, H.; Alcaraz, M. L.; Rubner, M. F.; Cohen, R. E. Zwitter-Wettability and Antifogging Coatings with Frost-Resisting Capabilities. *ACS Nano* **2013**, *7* (3), 2172−2185.

(12) Brown, P. S.; Atkinson, O.; Badyal, J. P. S. Ultrafast Oleophobic-Hydrophilic Switching Surfaces for Antifogging, Self-Cleaning, and Oil Water Separation. *ACS Appl. Mater. Interfaces* **2014**, *6* (10), 7504−7511.

(13) Zorba, V.; Chen, X. B.; Mao, S. S. Superhydrophilic TiO2 Surface Without Photocatalytic Activation. *Appl. Phys. Lett.* **2010**, *96* (9), 093702−093704.

(14) Li, Y. F.; Zhang, J. H.; Zhu, S. J.; Dong, H. P.; Jia, F.; Wang, Z. H.; Sun, Z. Q.; Zhang, L.; Li, Y.; Li, H. B.; Xu, W. Q.; Yang, B. Biomimetic Surfaces for High-Performance Optics. *Adv. Mater.* **2009**, *21* (46), 4731−4734.

(15) Lee, C. H.; Johnson, N.; Drelich, J.; Yap, Y. K. The Performance of Superhydrophobic and Superoleophilic Carbon Nanotube Meshes in Water-Oil Filtration. *Carbon* **2011**, *49* (2), 669−676.

(16) Wang, S. H.; Li, M.; Lu, Q. H. Filter Paper with Selective Absorption and Separation of Liquids that Differ in Surface Tension. *ACS Appl. Mater. Interfaces* **2010**, *2* (3), 677−683.

(17) Chen, G. H. Electrochemical Technologies in Wastewater Treatment. *Sep. Purif. Technol.* **2004**, *38* (1), 11−41.

(18) Xue, Z. X.; Cao, Y. Z.; Liu, N.; Feng, L.; Jiang, L. Special Wettable Materials for Oil/Water Separation. *J. Mater. Chem. A* **2014**, *2* (8), 2445−2460.

(19) Chen, P. C.; Xu, Z. K. Mineral-Coated Polymer Membranes with Superhydrophilicity and Underwater Superoleophobicity for Effective Oil/Water Separation. *Sci. Rep.* **2013**, *3*, 2776−2781.

(20) Jin, M. H.; Wang, J.; Yao, X.; Liao, M. Y.; Zhao, Y.; Jiang, L. Underwater Oil Capture by a Three-Dimensional Network Architectured Organosilane Surface. *Adv. Mater.* **2011**, *23* (25), 2861−2864.

(21) Xue, Z. X.; Wang, S. T.; Lin, L.; Chen, L.; Liu, M. J.; Feng, L.; Jiang, L. A Novel Superhydrophilic and Underwater Superoleophobic Hydrogel-Coated Mesh for Oil/Water Separation. *Adv. Mater.* **2011**, *23* (37), 4270−4273.

(22) Liu, Q. S.; Patel, A. A.; Liu, L. Y. Superhydrophilic and Underwater Superoleophobic Poly(sulfobetaine methacrylate)-Grafted Glass Fiber Filters for Oil-Water Separation. *ACS Appl. Mater. Interfaces* **2014**, *6* (12), 8996−9003.

(23) Zhang, F.; Zhang, W. B.; Shi, Z.; Wang, D.; Jin, J.; Jiang, L. Nanowire-Haired Inorganic Membranes with Superhydrophilicity and Underwater Ultralow Adhesive Superoleophobicity for High-Efficiency Oil/Water Separation. *Adv. Mater.* **2013**, *25* (30), 4192−4198.

(24) Kota, A. K.; Kwon, G.; Choi, W.; Mabry, J. M.; Tuteja, A. Hygro-responsive membranes for effective oil-water separation. *Nat. Commun.* **2012**, *3*, 1025.

(25) Gao, S. J.; Shi, Z.; Zhang, W. B.; Zhang, F.; Jin, J. Photoinduced Superwetting Single-Walled Carbon Nanotube/TiO2 Ultrathin Network Films for Ultrafast Separation of Oil-in-Water Emulsions. *ACS Nano* **2014**, *8* (6), 6344−6352.

(26) Estephan, Z. G.; Jaber, J. A.; Schlenoff, J. B. Zwitterion-Stabilized Silica Nanoparticles: Toward Nonstick Nano. *Langmuir* **2010**, *26* (22), 16884−16889.

(27) Yeh, S. B.; Chen, C. S.; Chen, W. Y.; Huang, C. J. Modification of Silicone Elastomer with Zwitterionic Silane for Durable Antifouling Properties. *Langmuir* **2014**, *30* (38), 11386−11393.

(28) Moulder, J. F.; Stickle, W. F.; Sobol, P. E.; Bomben, K. D. *Handbook of X-Ray Photoelectron Spectroscopy*; Perkin-Elmer: Boca Raton, FL, 1992.

(29) Yang, W. J.; Neoh, K. G.; Kang, E. T.; Lay-Ming Teo, S.; Rittschof, D. Stainless Steel Surfaces with Thiol-Terminated Hyperbranched Polymers for Functionalization via Thiol-Based Chemistry. *Polym. Chem.* **2013**, *4* (10), 3105−3115.

(30) Sin, M. C.; Sun, Y. M.; Chang, Y. Zwitterionic-Based Stainless Steel with Well-Defined Polysulfobetaine Brushes for General Bioadhesive Control. *ACS Appl. Mater. Interfaces* **2014**, *6* (2), 861−873.

(31) Liu, Q. S.; Li, W. C.; Wang, H.; Liu, L. Y. A Facile Method of Using Sulfobetaine-Containing Copolymers for Biofouling Resistance. *J. Appl. Polym. Sci.* **2014**, *131* (18), 40789−40797.

(32) Huang, C. J.; Chang, Y. C. In Situ Surface Tailoring with Zwitterionic Carboxybetaine Moieties on Self-Assembled Thin Film for Antifouling Biointerfaces. *Materials* **2014**, *7* (1), 130−142.

(33) Yu, B. Y.; Zheng, J.; Chang, Y.; Sin, M. C.; Chang, C. H.; Higuchi, A.; Sun, Y. M. Surface Zwitterionization of Titanium for a General Bio-Inert Control of Plasma Proteins, Blood Cells, Tissue Cells, and Bacteria. *Langmuir* **2014**, *30* (25), 7502−7512.

(34) Venault, A.; Yang, H. S.; Chiang, Y. C.; Lee, B. S.; Ruaan, R. C.; Chang, Y. Bacterial Resistance Control on Mineral Surfaces of Hydroxyapatite and Human Teeth via Surface Charge-Driven Antifouling Coatings. *ACS Appl. Mater. Interfaces* **2014**, *6* (5), 3201−3210.

(35) Jiang, S. Y.; Cao, Z. Q. Ultralow-Fouling, Functionalizable, and Hydrolyzable Zwitterionic Materials and Their Derivatives for Biological Applications. *Adv. Mater.* **2010**, *22* (9), 920−932.

(36) Zhang, Z.; Chao, T.; Chen, S. F.; Jiang, S. Y. Superlow Fouling Sulfobetaine and Carboxybetaine Polymers on Glass Slides. *Langmuir* **2006**, *22* (24), 10072−10077.

(37) Ye, S. H.; Johnson, C. A.; Woolley, J. R.; Murata, H.; Gamble, L. J.; Ishihara, K.; Wagner, W. R. Simple Surface Modification of a Titanium Alloy with Silanated Zwitterionic Phosphorylcholine or Sulfobetaine Modifiers to Reduce Thrombogenicity. *Colloids Surf., B* **2010**, *79* (2), 357−364.

(38) Estephan, Z. G.; Hariri, H. H.; Schlenoff, J. B. One-Pot, Exchange-Free, Room-Temperature Synthesis of Sub-10 nm Aqueous, Noninteracting, and Stable Zwitterated Iron Oxide Nanoparticles. *Langmuir* **2013**, *29* (8), 2572−2579.

(39) Zhang, L. B.; Zhong, Y. J.; Cha, D.; Wang, P. A Self-Cleaning Underwater Superoleophobic Mesh for Oil-Water Separation. *Sci. Rep.* **2013**, *3*, 2326.

(40) Litt, M.; Matsuda, T. Siloxane Zwitterions: Synthesis and Surface Properties of Crosslinked Polymers. *J. Appl. Polym. Sci.* **1975**, *19* (5), 1221−1225.

DOI: 10.1021/acsami.5b07362
ACS Appl. Mater. Interfaces 2015, 7, 21021−21029

(41) Rezaei, B.; Havakeshian, E.; Ensafi, A. A. Stainless steel modified with an aminosilane layer and gold nanoparticles as a novel disposable substrate for impedimetric immunosensors. *Biosens. Bioelectron.* **2013**, *48*, 61−66.
(42) Peng, X. S.; Jin, J.; Nakamura, Y.; Ohno, T.; Ichinose, I. Ultrafast Permeation of Water Through Protein-Based Membranes. *Nat. Nanotechnol.* **2009**, *4* (6), 353−357.
(43) Gao, M.; Gawel, K.; Stokke, B. T. Polyelectrolyte and Antipolyelectrolyte Effects in Swelling of Polyampholyte and Polyzwitterionic Charge Balanced and Charge Offset Hydrogels. *Eur. Polym. J.* **2014**, *53*, 65−74.
(44) Zhang, Z.; Vaisocherova, H.; Cheng, G.; Yang, W.; Xue, H.; Jiang, S. Y. Nonfouling Behavior of Polycarboxybetaine-Grafted Surfaces: Structural and Environmental Effects. *Biomacromolecules* **2008**, *9* (10), 2686−2692.

DOI: 10.1021/acsami.5b07362
ACS Appl. Mater. Interfaces 2015, 7, 21021−21029